

Auditing Combinatorial Randomness from Finite Transcripts

Faruk Alpay* Levent Sarioglu

Department of Computer Engineering, Bahcesehir University, Istanbul, Turkey
 faruk.alpay@bahcesehir.edu.tr, levent.sarioglu@bahcesehir.edu.tr

*Correspondence: alpay@lightcap.ai

Abstract

Public randomness services expose finite transcripts: lottery histories, randomness-beacon pulses, and generator audit streams. A transcript auditor must control false alarms under the public null while retaining power against tampering or implementation faults. For combinatorial draws without replacement, the transcript space has support size $\binom{m}{k}$, and arbitrary joint-uniformity testing inherits the sparse-uniformity barrier $\Theta(\sqrt{\binom{m}{k}}/\varepsilon^2)$. We formulate this barrier as a black-box auditability frontier and construct generator-agnostic geometric audits for structured alternatives. The battery maps draws to the hypersimplex and evaluates exact-combinatorial null calibrated statistics: marginal chi-square, pair maxima, serial overlap, anchored-box discrepancy, and low-dimensional H0/MST geometry. On 1,956 EuroMillions main-number draws from 2004-02-13 through 2026-06-19, no statistic survives false-discovery adjustment among observed/reference sources (minimum observed/reference BH $q = 0.279$). In contrast, GPU Monte Carlo experiments with up to 300,000 exact-null replications and 60,000 alternative replications per condition show that marginal-preserving joint alternatives are invisible to one-dimensional marginal tests while being detected by geometric/pair statistics. For a 5/50 draw at $n = 1,956$, a block-cluster alternative of strength 0.04 is detected by pair maxima with power 0.638 while marginal chi-square remains at 0.051; a band-repulsion alternative of strength 0.08 is detected by anchored boxes with power 0.741 while marginal chi-square remains at 0.051. The results separate marginal goodness-of-fit from joint-structure audit power and quantify the sample sizes at which specified low-dimensional failure modes become detectable.

1 Introduction

Public randomness is a security primitive when multiple parties rely on a source whose internal entropy is not directly observable. Lotteries, public randomness beacons, and deployed pseudorandom generators all leave audit transcripts; the security-relevant object is the finite transcript and the class of deviations it can rule out. For a draw of k labels without replacement from m , the exact null distribution is uniform on

$$\Omega_{m,k} = \{x \in \{0,1\}^m : \|x\|_1 = k\}, \quad |\Omega_{m,k}| = \binom{m}{k}.$$

The main EuroMillions component has $\binom{50}{5} = 2,118,760$ possible outcomes, while a 6/90 format has 622,614,630. Single-coordinate count tests see only a projection of this space. A distribution can preserve every single-number marginal and still alter pair probabilities, serial overlap, or the geometry of sorted draws.

The security limitation is information-theoretic. Any black-box transcript audit for arbitrary alternatives on $\Omega_{m,k}$ inherits Paninski’s uniformity-testing scale, so lottery-length transcripts cannot

certify full joint uniformity without restricting the adversary or fault model. The constructive route is to audit named structured families: hot labels, pair couplings, serial stickiness, clustered blocks, and band repulsion. These families model low-dimensional tampering or implementation faults and can be tested by exact-null calibrated geometric statistics.

The contributions are:

1. A transcript-audit model for public combinatorial randomness, with audit advantage defined against a named alternative class.
2. A lower-bound corollary showing that arbitrary joint-uniformity audits require $\Omega(\sqrt{\binom{m}{k}}/\varepsilon^2)$ samples.
3. Generator-agnostic statistics on the draw hypersimplex: marginal counts, pair maxima, serial overlap, anchored-box discrepancy, and H0/MST geometry. The anchored boxes are calibrated against the exact combinatorial model.
4. CPU and CUDA implementations, with GPU experiments on an NVIDIA RTX 5090 and an NVIDIA A100 SXM4. The GPU experiments add marginal-preserving alternatives that directly expose the blind spot of one-dimensional audits.

2 Related Work

Classical RNG testing has a mature empirical tradition, including TestU01 [12]. Lattice, spectral, and discrepancy methods connect random-number generation to geometry and quasi-Monte Carlo theory [14]. These tests are especially powerful for structured linear generators. The present setting is black-box: the input is a finite sequence of combinatorial draws, with no access to a generator recurrence. For cryptographic random-bit generation, NIST SP 800-22 provides statistical tests for output streams and SP 800-90B specifies validation requirements for entropy sources [1, 17]. Statistical transcript auditing addresses observable distributional faults; it is distinct from computational unpredictability and from implementation-level entropy claims.

Distribution testing gives the relevant lower-bound scale. Paninski’s coincidence test and matching lower bound show that uniformity over a support of size N requires $\Theta(\sqrt{N}/\varepsilon^2)$ samples for constant success probability in total variation distance [15]. The implication for draws without replacement is immediate once $N = \binom{m}{k}$. Canonne’s survey gives the broader property-testing context for these sample-complexity barriers [4]. The applied statistical treatment of coincidences has a parallel tradition in audit problems, including the birthday-style methods of Diaconis and Mosteller [6].

Computational geometry enters through discrepancy and topological summaries. Exact star discrepancy is computationally hard in high dimension [9], motivating finite, calibrated families of anchored boxes rather than exact high-dimensional optimization. Topological data analysis provides statistically meaningful summaries such as persistence landscapes [3], with standard algorithmic foundations in computational topology [7, 8]. Random geometric complexes give null theory for geometric point clouds [2]. GPU persistent homology systems such as Ripser++ demonstrate that these computations can be scaled [19]. The H0 statistic used below is exactly the Euclidean minimum-spanning-tree edge spectrum in the projected draw cloud.

Public randomness beacons are becoming more auditable. The NIST beacon format specifies signed, timestamped pulses and interoperability goals [11]. CURBy is a public beacon based on traceable quantum randomness [10, 18]; our data script cached 16,000 bytes from 250 completed

CURBy rounds during the 2026-06-20 run. EuroMillions draws were obtained from the public EuroMillions API repository [13]; the local cache contains 1,956 main-number draws.

3 Security Model and Auditability Frontier

Definition 1 (Transcript auditor). *Let U be the uniform law on $\Omega_{m,k}$. A randomized transcript auditor is a map $A : \Omega_{m,k}^n \rightarrow \{0, 1\}$, where $A = 1$ denotes rejection. It has level α if $\Pr_{U^n}(A = 1) \leq \alpha$. Its audit advantage against a source law P is*

$$\text{Adv}_A(P) = \Pr_{P^n}(A = 1) - \Pr_{U^n}(A = 1).$$

Definition 2 (Arbitrary-alternative radius). *Let $N = \binom{m}{k}$. The sparse-uniformity scale for arbitrary alternatives is*

$$\varepsilon_{\text{arb}}(m, k, n) = \left(\frac{\sqrt{N}}{n} \right)^{1/2}.$$

It is the total-variation separation obtained by solving $n \asymp \sqrt{N}/\varepsilon^2$ for ε .

Theorem 1 (Black-box audit lower bound). *Fix constants $\alpha, \beta \in (0, 1/2)$ and let*

$$\mathcal{P}_\varepsilon = \{P : \text{TV}(P, U) \geq \varepsilon\}.$$

If a level- α auditor satisfies $\inf_{P \in \mathcal{P}_\varepsilon} \Pr_{P^n}(A = 1) \geq 1 - \beta$, then

$$n = \Omega_{\alpha, \beta} \left(\frac{\sqrt{\binom{m}{k}}}{\varepsilon^2} \right).$$

This order is achievable up to constants by sparse-uniformity testing.

Proof. Set $N = \binom{m}{k}$ and identify each draw with one of the N atoms in $\Omega_{m,k}$. The statement is Paninski's minimax uniformity-testing lower and upper scale applied to this induced discrete distribution [15]. \square

For 5/50, $\sqrt{N} = 1,456$ and $n = 1,956$ gives the constant-one separation scale $\varepsilon \approx \sqrt{\sqrt{N}/n} = 0.863$. For 6/49 with $n = 2,300$, the same calculation is 1.275; for 6/90 with $n = 1,000$, it is 4.995, outside the range of total variation. No level-controlled black-box auditor can offer uniform power over all separated source laws at these transcript lengths.

Proposition 1 (Marginal non-identifiability). *For $2 \leq k \leq m-2$, there are non-uniform distributions on $\Omega_{m,k}$ with exactly uniform single-coordinate marginals.*

Proof. Choose four distinct labels a, b, c, d . For $S \in \Omega_{m,k}$ define

$$h(S) = \mathbf{1}\{a, b \subset S\} + \mathbf{1}\{c, d \subset S\} - \mathbf{1}\{a, c \subset S\} - \mathbf{1}\{b, d \subset S\}.$$

The sum of $h(S)$ over all S is zero. Conditioning on any fixed label also gives zero: for labels in $\{a, b, c, d\}$ the positive and negative terms cancel, and for any other label all four terms have the same count $\binom{m-3}{k-3}$, with the convention that this count is zero when $k = 2$. Hence, for sufficiently small $|\theta|$,

$$P_\theta(S) = \binom{m}{k}^{-1} \{1 + \theta h(S)\}$$

is a valid non-uniform distribution whose single-coordinate marginals match the uniform law. Pair probabilities are changed whenever $\theta \neq 0$. \square

Theorem 2 (Structured witness audit). Let $\mathcal{F} = \{f_1, \dots, f_L\}$ with $f_j : \Omega_{m,k} \rightarrow [0, 1]$, let $\mu_j = \mathbb{E}_U f_j(X)$, and define

$$D_{\mathcal{F}} = \max_{1 \leq j \leq L} \left| \frac{1}{n} \sum_{i=1}^n f_j(X_i) - \mu_j \right|.$$

The threshold

$$\tau_{\alpha} = \sqrt{\frac{\log(2L/\alpha)}{2n}}$$

defines a level- α auditor. If $\Delta_{\mathcal{F}}(P) = \max_j |\mathbb{E}_P f_j - \mu_j|$ satisfies

$$\Delta_{\mathcal{F}}(P) \geq \tau_{\alpha} + \sqrt{\frac{\log(2/\beta)}{2n}},$$

then the rejection probability under P is at least $1 - \beta$.

Proof. Under U^n , Hoeffding's inequality and a union bound over the L witnesses give $\Pr_{U^n}(D_{\mathcal{F}} > \tau_{\alpha}) \leq \alpha$. Let f_{j^*} attain the witness gap under P . A second Hoeffding bound places its empirical mean within $\sqrt{\log(2/\beta)/(2n)}$ of its P -expectation with probability at least $1 - \beta$; the displayed gap then forces rejection. \square

Anchored boxes use witnesses $f_t(y) = \mathbf{1}\{y \leq t\}$. Pair indicators and bounded serial-overlap functions give analogous auditors. Their sample requirements depend on the witness gap and $\log L$, rather than directly on the full support size $\binom{m}{k}$.

Lemma 1 (Exact Monte Carlo calibration). Let T be any statistic whose large values are more extreme, and let $T_0^{(1)}, \dots, T_0^{(B)}$ be i.i.d. exact-null replications generated at the same (m, k, n) as the observed sample. The randomized-rank p -value

$$\hat{p} = \frac{1 + \sum_{b=1}^B \mathbf{1}\{T_0^{(b)} \geq T_{\text{obs}}\}}{B + 1}$$

satisfies $\Pr_{H_0}(\hat{p} \leq \alpha) \leq \alpha$ for every $\alpha \in [0, 1]$.

Proof. Under H_0 , $T_{\text{obs}}, T_0^{(1)}, \dots, T_0^{(B)}$ are exchangeable. The rank of T_{obs} among the $B + 1$ values is therefore uniform up to ties; using the upper-tail count with the additive one is the standard conservative tie handling. \square

Lemma 2 (Null moments for pair and serial statistics). For a fixed unordered pair $\{i, j\}$, the per-draw inclusion probability is

$$p_2 = \Pr(i, j \in X) = \frac{k(k-1)}{m(m-1)}.$$

Thus its count over n independent draws is Binomial(n, p_2) marginally. For two consecutive independent draws, $|X_t \cap X_{t-1}|$ is hypergeometric with

$$\mathbb{E}|X_t \cap X_{t-1}| = \frac{k^2}{m}, \quad \text{Var}(|X_t \cap X_{t-1}|) = k \frac{k}{m} \left(1 - \frac{k}{m}\right) \frac{m-k}{m-1}.$$

Proof. The pair probability follows by sampling two named labels without replacement. For the overlap, condition on X_{t-1} . The next draw samples k labels from a population of size m containing k marked labels, giving the displayed hypergeometric moments [5, 16]. \square

4 Methods

Exact null. Every null sample is drawn without replacement from $\{1, \dots, m\}$ and sorted. Let $Y = (Y_{(1)}, \dots, Y_{(k)})$ be the sorted zero-indexed labels. For an anchored threshold vector $t = (t_1, \dots, t_k)$, the exact null probability is

$$q_t = \binom{m}{k}^{-1} \#\{0 \leq y_1 < \dots < y_k < m : y_j \leq t_j \forall j\}.$$

The CUDA implementation evaluates this count by dynamic programming:

$$C(r, a) = \sum_{v=a}^{\min(t_r, m-k+r)} C(r+1, v+1), \quad C(k, a) = 1,$$

with $q_t = C(0, 0) / \binom{m}{k}$. This avoids a continuous-uniform approximation for the sorted simplex.

Statistics. We report five statistic families:

- marginal chi-square, $\sum_{i=1}^m (C_i - nk/m)^2 / (nk/m)$;
- pair max-z, $\max_{i < j} |(C_{ij} - np_2) / \sqrt{np_2(1-p_2)}|$;
- serial overlap-z, based on the hypergeometric moments above;
- anchored-box discrepancy, $\max_{t \in \mathcal{T}} |n^{-1} \sum_{\ell=1}^n \mathbf{1}\{Y_\ell \leq t\} - q_t|$;
- H0/MST geometry, obtained by projecting incidence vectors with a fixed Gaussian map and summarizing the Euclidean minimum-spanning-tree edge spectrum.

The maximum statistics are calibrated by exact-null Monte Carlo, so dependence among pairs or boxes is kept in the reference distribution.

Alternative families. We use five controlled alternatives:

- hot-marginal: a low-index subset receives multiplicative sampling weight;
- pair-injection: a fixed pair is injected with probability ρ ;
- block-cluster: with probability ρ , choose one of m/k blocks and return that whole block; single-number marginals remain uniform;
- band-repulsion: with probability ρ , choose one number from each of k equal bands; single-number marginals remain uniform;
- serial-stickiness: with probability ρ , copy one label from the previous draw and fill the rest uniformly.

Calibration. All p-values and power values are Monte Carlo calibrated at the same sample size as the tested source. The local source audit used 300 null replications. The GPU experiments used 50,000–100,000 null replications per n and 10,000–20,000 alternative replications per condition in the first pass, with larger calibrated replications for the final GPU tables. Discrete statistics use conservative upper-tail rejection against the calibrated critical value to avoid size inflation from ties.

5 Results

5.1 Observed and Reference Sources

The local source audit uses EuroMillions main-number draws from 2004-02-13 through 2026-06-19, plus PCG64, MT19937, a weak LCG, controlled alternatives, and a small CURBy cache. Table 1 reports calibrated p-values. For the observed EuroMillions source, the minimum p-value is 0.106. Among the observed/reference sources, the minimum Benjamini–Hochberg q-value is 0.279. The EuroMillions trace is inside the calibrated reference range of this battery.

statistic source	marginal_chi2	pair_max_z	serial_overlap_z	anchored_box	projection_energy	mst_cv	h0_total_persistence
curby_qrng_beacon	0.030	0.475	0.339	0.020	0.342	0.641	0.801
euromillions_main	0.163	0.944	0.834	0.515	0.106	0.282	0.522
lcg_minstd	0.189	0.751	0.774	0.040	0.578	0.156	0.807
mt19937_reference	0.013	0.120	0.854	0.944	0.661	0.316	0.425
pair_bias_0.12	0.003	0.003	0.439	0.003	0.811	0.080	0.093
pcg64_reference	0.721	0.751	0.970	0.764	0.080	0.794	0.123
sticky_0.16	0.468	0.751	0.003	0.369	0.306	0.914	0.269
weighted_hot_0.45	0.003	0.003	0.003	0.003	0.924	0.312	0.797

Table 1: Calibrated p-values from the local source audit. The CURBy row is limited by the 16,000-byte cache available during the run ($n = 280$ converted 5/50 draws). EuroMillions has $n = 1,956$ main-number draws.

5.2 Marginal-Preserving Alternatives

At $n = 1,956$, the two marginal-preserving alternatives keep marginal chi-square near nominal size while joint/geometric tests gain power (Figure 1). Under block clustering at strength 0.04, pair max-z reaches 0.638 power while marginal chi-square is 0.051. Under band repulsion at strength 0.08, anchored boxes reach 0.741 power while marginal chi-square is 0.051.

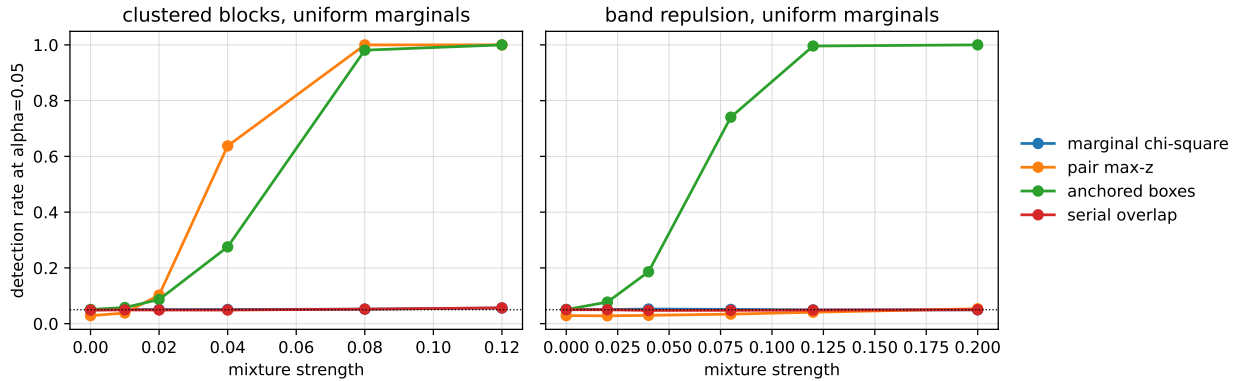


Figure 1: Marginal-preserving alternatives at $n = 1,956$ for 5/50 draws. The single-number marginal test remains at nominal size, while pair and geometric statistics detect joint structure.

5.3 Sample-Size Frontier

Figure 2 fixes the alternative strength at 0.04 and varies the number of draws. The transition is gradual: for block clustering, pair max-z power is 0.638 at $n = 1,956$ and 0.999 at $n = 5,000$, while

marginal chi-square stays near 0.05. For band repulsion, anchored-box power is 0.186 at $n = 1,956$, 0.489 at $n = 5,000$, 0.882 at $n = 10,000$, 0.971 at $n = 12,000$, and 1.000 at $n = 20,000$. The same structured deviation can therefore have low audit advantage at one transcript length and near-unit detection probability at a larger one.

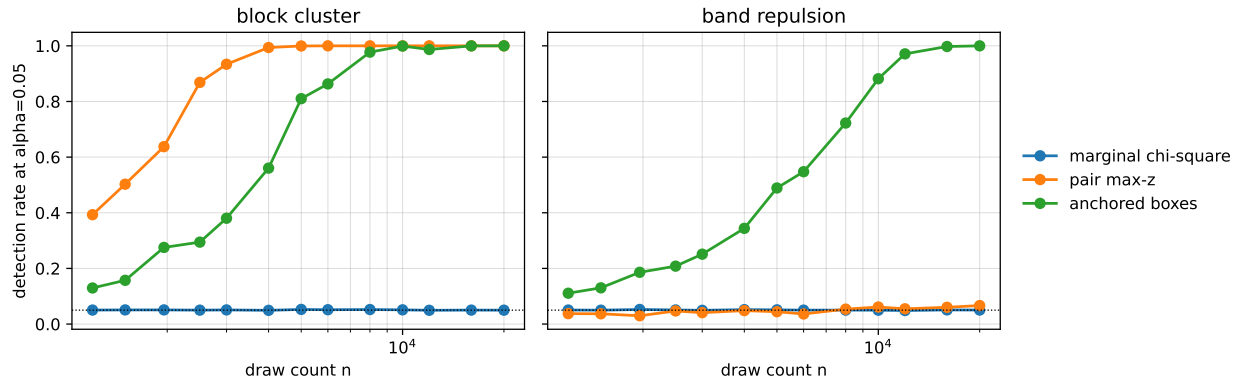


Figure 2: Sample-size frontier for marginal-preserving alternatives at strength 0.04 in 5/50 draws. The x-axis is logarithmic.

5.4 Format Scale

The fixed 6/54 run and the A100 6/90 run repeat the GPU audit for larger supports, including $C(90, 6) = 622,614,630$. At $n = 5,000$, 6/90 block-cluster strength 0.04 is detected by pair max-z with power 1.000 and by anchored boxes with power 0.688, while marginal chi-square is 0.049. For 6/90 band-repulsion strength 0.04, anchored boxes reach 0.651 power, while marginal chi-square is 0.048 and pair max-z is 0.051. The fixed 6/54 run gives the same pattern at $n = 5,000$: block clustering has pair max-z power 1.000 and anchored box power 0.606, while band repulsion has anchored-box power 0.712 and marginal chi-square remains 0.053. Figure 3 compares 5/50, 6/54, and 6/90 surfaces.

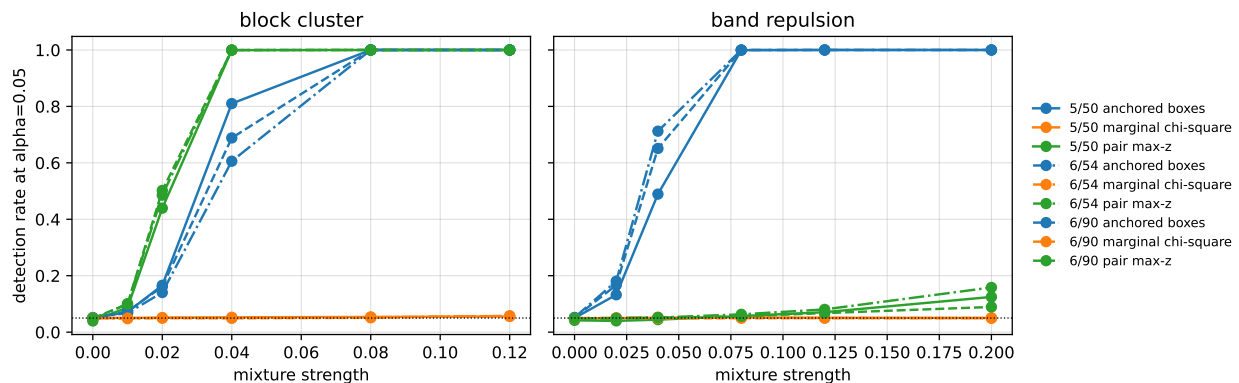


Figure 3: Format-scale comparison at $n = 5,000$. Solid lines are 5/50, dash-dotted lines are 6/54, and dashed lines are 6/90. Marginal-preserving alternatives keep marginal chi-square near nominal size across formats.

6 Discussion

The experiments separate three regimes. First, arbitrary joint uniformity is outside the information budget of real lottery histories. Second, marginal-only audits can be exactly blind to meaningful joint alternatives. Third, geometric and pair statistics have useful power against stated alternatives, especially as the audit sample grows.

Each reported value is attached to a source, null model, alternative class, statistic, calibration budget, and power curve. These elements define the scope of the finite-transcript security claim and can be reproduced from the archived code and CSV files.

Limitations. The CPU H0/MST statistic is deliberately modest; full H1/H2 persistent homology would require an additional Ripser++-style pipeline. The CURBy cache used in the source table is small because the public endpoint was slow during the run; it is included as a low-volume reference-source smoke test. An early 6/54 exploratory run exposed an anchored-box implementation issue and was discarded. The archived 6/54 CSV, main tables, and figures use the corrected implementation.

7 Reproducibility

All code, cached public data, generated figures, final GPU CSV files, and result tables are included in the ancillary archive. A SHA-256 artifact manifest records the packaged files. The main commands are:

```
python3 scripts/fetch_data.py
python3 scripts/run_experiments.py
nvcc -O3 -std=c++17 scripts/gpu_combinatorial_audit.cu -lcurand \
  -o build/gpu_combinatorial_audit
python3 scripts/analyze_gpu_results.py
```

The GPU CSV files record device label, n , alternative, strength, statistic, replication count, critical value, null mean/standard deviation, wall-clock seconds, box count, and seed.

8 Conclusion

Full joint uniformity over $\Omega_{m,k}$ has the $\sqrt{\binom{m}{k}}$ sparse-testing barrier. Structured witness families avoid direct dependence on the full support and require $O((\log L + \log(1/\beta))/\Delta^2)$ samples for witness gap Δ . Exact-null calibrated marginal, pair, serial, and geometric auditors instantiate this security tradeoff for finite combinatorial transcripts.

References

- [1] Lawrence E. Bassham, Andrew L. Rukhin, Juan Soto, James R. Nechvatal, Miles E. Smid, Elaine B. Barker, Stefan D. Leigh, Mark Levenson, Mark Vangel, David L. Banks, Nathanael Alan Heckert, James F. Dray, and San Vo. A statistical test suite for random and pseudorandom number generators for cryptographic applications. Special Publication 800-22 Revision 1a, National Institute of Standards and Technology, 2010.

- [2] Omer Bobrowski and Matthew Kahle. Topology of random geometric complexes: A survey. *Journal of Applied and Computational Topology*, 1(3–4):331–364, 2018. doi: 10.1007/s41468-017-0010-0.
- [3] Peter Bubenik. Statistical topological data analysis using persistence landscapes. *Journal of Machine Learning Research*, 16(3):77–102, 2015. URL <https://jmlr.org/papers/v16/bubenik15a.html>.
- [4] Clément L. Canonne. A survey on distribution testing: Your data is big. but is it blue? *Theory of Computing*, pages 1–100, 2020. doi: 10.4086/toc.gs.2020.009. URL <https://theoryofcomputing.org/articles/g009/>. Graduate Surveys 9.
- [5] Vasek Chvatal. The tail of the hypergeometric distribution. *Discrete Mathematics*, 25(3): 285–287, 1979. doi: 10.1016/0012-365X(79)90084-0.
- [6] Persi Diaconis and Frederick Mosteller. Methods for studying coincidences. *Journal of the American Statistical Association*, 84(408):853–861, 1989. doi: 10.1080/01621459.1989.10478847.
- [7] Herbert Edelsbrunner and John Harer. *Computational Topology: An Introduction*. American Mathematical Society, Providence, RI, 2010. ISBN 9780821849255.
- [8] Robert Ghrist. Barcodes: The persistent topology of data. *Bulletin of the American Mathematical Society*, 45(1):61–75, 2008. doi: 10.1090/S0273-0979-07-01191-3.
- [9] Michael Gnewuch, Anand Srivastav, and Carola Winzen. Finding optimal volume subintervals with k points and calculating the star discrepancy are NP-hard problems. *Journal of Complexity*, 25(2):115–127, 2009. doi: 10.1016/j.jco.2008.07.001.
- [10] Gautam A. Kavuri, Jasper Palfree, Dileep V. Reddy, Yanbao Zhang, Joshua C. Bienfang, Michael D. Mazurek, et al. Traceable random numbers from a non-local quantum advantage. *Nature*, 2025. doi: 10.1038/s41586-025-09054-3.
- [11] John Kelsey, Luís T. A. N. Brandão, Rene Peralta, and Harold Booth. A reference for randomness beacons: Format and protocol version 2. Draft NISTIR 8213, National Institute of Standards and Technology, 2019.
- [12] Pierre L’Ecuyer and Richard Simard. TestU01: A C library for empirical testing of random number generators. *ACM Transactions on Mathematical Software*, 33(4):22, 2007. doi: 10.1145/1268776.1268777.
- [13] Pedro Mealha. Euromillions public API. <https://github.com/pedro-mealha/euromillions-api>, 2026. Accessed 2026-06-20.
- [14] Harald Niederreiter. *Random Number Generation and Quasi-Monte Carlo Methods*. SIAM, Philadelphia, 1992. doi: 10.1137/1.9781611970081.
- [15] Liam Paninski. A coincidence-based test for uniformity given very sparsely sampled discrete data. *IEEE Transactions on Information Theory*, 54(10):4750–4755, 2008. doi: 10.1109/TIT.2008.928987.
- [16] Robert J. Serfling. Probability inequalities for the sum in sampling without replacement. *The Annals of Statistics*, 2(1):39–48, 1974. doi: 10.1214/aos/1176342611.

- [17] Meltem Sönmez Turan, Elaine Barker, John Kelsey, Kerry A. McKay, Mary L. Baish, and Mike Boyle. Recommendation for the entropy sources used for random bit generation. Special Publication 800-90B, National Institute of Standards and Technology, 2018.
- [18] University of Colorado Boulder. CURBy: CU randomness beacon. <https://random.colorado.edu/>, 2026. Accessed 2026-06-20.
- [19] Simon Zhang, Mengbai Xiao, and Hao Wang. GPU-accelerated computation of Vietoris–Rips persistence barcodes. In *36th International Symposium on Computational Geometry (SoCG 2020)*, volume 164 of *Leibniz International Proceedings in Informatics (LIPIcs)*, pages 70:1–70:17. Schloss Dagstuhl – Leibniz-Zentrum für Informatik, 2020. doi: 10.4230/LIPIcs.SoCG.2020.70.